Theoretical Investigation of the Reaction of $ClONO_2$ with H_2O on Water Clusters

Si Chuan Xu and Xin Sheng Zhao*

Department of Chemistry, Peking University, Beijing 100871, China

Received: March 6, 1998; In Final Form: June 22, 1998

The reaction of $ClONO_2$ with H_2O on various water clusters has been investigated via an ab initio calculation at the MP2//HF/6-31G(d) level. The calculations have shown that as more water molecules are involved in the reaction, the barrier height drops dramatically. The barrier energies of the reaction on the water clusters vary with the extent of hydration. A value as low as 3.2 kcal/mol was observed in the calculation. It is suggested that the ice surface shows catalytic character for the heterogeneous reaction through structure catalysis and hydration. It is shown that our mechanism of $ClONO_2$ hydrolysis on ice surfaces is in a broad sense compatible with the ion-catalyzed mechanism.

I. Introduction

The heterogeneous reaction of $ClONO_2$ with H_2O readily occurs on polar stratospheric clouds (PSCs), even though in the gas phase $ClONO_2$ is a stable molecule. This reaction has been extensively studied experimentally and theoretically.[1−18] Two kinds of seemingly different mechanisms have been proposed.[9,19−33] In the ion-catalyzed mechanism, ionization or dissociation of the reactant is thought to play a central role. H^+ or other ions help the ionization of the reactant. The mechanism proposed by Sodeau and co-workers emphasizes the importance of ionization of the reactant from hydration.[16,31,32] In this kind of mechanism, the role of the ice structure in the reaction is not given enough attention. Hanson presented a study of reactivity of $ClONO_2$ on $H_2{}^{18}O$ ice and organic liquids.[24] The study suggested that neither ionization nor dissociation are prerequisites for heterogeneous reactions of $ClONO_2$. The reaction of $ClONO_2$ on liquid organic surfaces also is efficient.[24] The second kind of mechanism, which we called the multimolecule-formed transition state (MTS) mechanism,[29,30,33] emphasizes the importance of the ice structure,[25] and was independently proposed by our group[25,29,30,33] and by the Hynes group.[26] For convenience, we call this second kind of mechanism a structure-catalyzed mechanism. Very recently, Sodeau and co-workers presented experimental evidence for the second kind of mechanism at low temperature,[32] but they argued in another paper that ionization prevails at the atmospherically interesting condition.[31]

The heterogeneous reaction of $ClONO_2$ hydrolysis is quite complex. Many factors such as particle size and structure of surface, reactant-to-water ratio, available free water, and temperature affect the reaction. In our view, the two models of ion-catalyzed and structure-catalyzed mechanisms have emphasized two different aspects of the reaction. A view combining both the models probably is better suited to explain the known experimental facts. It is the purpose of this paper to show through a theoretical investigation that the two models are compatible. Also, a better understanding of experimental observations can be achieved through the combination of the two models.

II. Methods of Calculation

To make a theoretical investigation tractable, we focus our attention on the reaction on water clusters as our model system. Similar to the strategy used by us before,[29,30,33] the following reactions on water clusters are considered:

$$\begin{aligned}&\{ClONO_2 + (H_2O)_\alpha\cdot H_2O\cdot(H_2O)_\beta\}\ (R) \rightarrow\\&\qquad \{ClONO_2\cdot(H_2O)_\alpha\cdot H_2O\cdot(H_2O)_\beta\}\ (RC) \rightarrow\\&\qquad [ClONO_2\cdot(H_2O)_\alpha\cdot H_2O\cdot(H_2O)_\beta]^\ddagger\ (TS) \rightarrow\\&\qquad \{HONO_2\cdot(H_2O)_\alpha\cdot HOCl\cdot(H_2O)_\beta\}\ (PC) \rightarrow\\&\qquad \{HONO_2\cdot(H_2O)_\alpha\cdot(H_2O)_\beta + HOCl\}\ (P)\ \alpha =\\&\qquad\qquad 0,1,2 \text{ and } 3,\ \beta = 0,1,2 \quad (1)\end{aligned}$$

In the reaction, α water molecules form a ring with the reactants, and β water molecules attach to the ring. R is the reactant; RC, the reactant complex; PC, the product complex; TS, the transition state; and P, the final product. When both α and $\beta = 0$, it resembles the gas-phase reaction, and when α increases from 0 to 3 while keeping $\beta = 0$, it aims at understanding the role of the water molecules in the ring. After having considered the ice structure[26] and to avoid computational difficulty, we chose the case of three water molecules in the ring ($\alpha = 2$) to investigate further the effect of hydration of the ring by additional water molecules ($\beta = 1,2$).

The geometry optimization, energy calculation, vibrational analysis, and zero-point energy (ZPE) correction were done with the Gaussian 94 programs.[34] The stable geometries were optimized, and confirmed by the vibrational analysis where no imaginary frequency was found. The transition states were automatically searched after RC and PC were found, and were also confirmed by the vibrational analysis with one and just one imaginary frequency and the corresponding vibrational mode being coincident with the reaction coordinate.

To consistently treat reaction 1 for all different α and β values, we chose MP2//HF/6-31G(d) level calculations. To check the MP2//HF/6-31G(d) level, the comparisons of the calculations between the MP2//HF/6-31G(d) and MP2/6-31G(d) levels were made. Table 1 presents the ZPE-corrected relative energies for reaction 1, $\alpha, \beta = 0$. The agreement was

10.1021/jp9814045 CCC: $18.00 © 1999 American Chemical Society
Published on Web 03/13/1999

TABLE 1: Comparison of ZPE-Corrected Relative Energies (kcal/mol) Calculated by Different Theoretical Methods for Reaction of $ClONO_2$ with H_2O, Reactants as Reference

	R	RC	TS	PC	P
MP2//HF/6-31G(d)	0	−4.8	63.3	−5.7	0.7
MP2/6-31G(d)	0	−4.0	67.8	−3.8	3.1

TABLE 2: Comparison of Geometry Parameters among Different Theoretical Methods and Experimental Data[a]

parameter	HF/ 631G(d)	MP2/ 6-31G(d)	B3LYP/ 6-311G(d,p)[25]	CCSD(T)/ TZ2P[35]	expt[36]
$ClONO_2$					
r_{Cl-O}	1.666	1.703	1.717	1.707	1.673
r_{O-N}	1.372	1.547	1.516	1.511	1.499
r_{N-O}	1.172	1.203	1.186	1.195	1.196
r_{N-O}	1.172	1.203	1.188	1.197	1.196
$\angle_{ClON}$	115.7	111.1	113.6	111.9	113.0
$\angle_{ONO}$	118.6	117.3	117.7	117.8	118.6
$\angle_{ONO}$	110.7	107.6	108.2	108.7	108.8
HNO_3					
r_{H-O}	0.955	0.983	0.971	0.969	0.964
r_{O-N}	1.334	1.412	1.415	1.418	1.406
r_{N-O}	1.188	1.226	1.210	1.216	1.211
r_{N-O}	1.172	1.216	1.194	1.200	1.199
$\angle_{HON}$	105.3	102.1	103.0	101.5	102.2
$\angle_{ONO}$	116.1	115.8	115.6	115.4	115.9
$\angle_{ONO}$	114.8	113.6	113.9	114.0	113.9

[a] Bond length in Å, bond angle in deg.

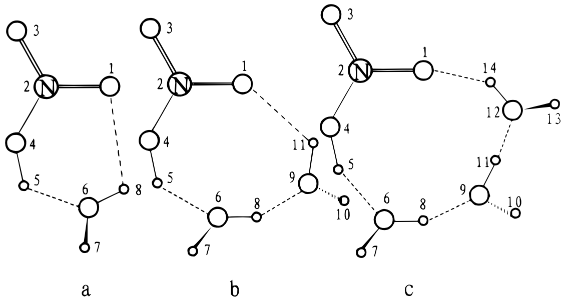

Figure 1. Optimized geometries of $HNO_3 \cdot (H_2O)_\alpha$, $\alpha = 1$ (a), 2 (b), 3 (c) at the HF/6-31G(d) level.

quite good in relative energies between MP2//HF/6-31G(d) and MP2/6-31G(d) levels. When $\alpha, \beta = 0$, the value of the reaction energy is similar to that of the reaction enthalpy, because the molarity does not change in the reaction. The calculated energies, 0.7 kcal/mol at the MP2//HF/6-31G(d) level and 3.1 kcal/mol at the MP2/6-31G(d) level, are consistent with the experimental enthalpy of 2 ± 3 kcal/mol.[15] Table 2 presents the comparison of the geometry data among the HF/6-31G(d), MP2/6-31G(d), other levels from the literature, and the experimental values for $ClONO_2$ and HNO_3. It is noticed that the agreement is good in general. The following discussions will focus on the MP2//HF/6-31G(d) level calculations only.

III. Results and Discussion

A. Structure and Energy of the Ring Only. *a. Optimized Geometries. Reactant and Product Structures.* The stable ring structures were assumed to be reactant and product, respectively. All structures designed in reaction 1 were found. The optimized geometries of $(H_2O)_\alpha \cdot H_2O$ (R) $\alpha = 0$, 1, 2, and 3 are similar to those found by Xantheas and Dunning.[37] Figure 1 shows the optimized geometries of $HONO_2 \cdot (H_2O)_\alpha$ (P) $\alpha = 1$, 2, and 3 marked as a, b, and c, respectively. Their bond lengths and some of bond angles are presented in Table 3. The values of r_{O4-H5} are 0.972, 0.979, and 0.981 Å, whereas those of r_{H5-O6}, 1.768, 1.703, and 1.686 Å for a, b, and c configurations, respectively. The calculated result shows that ionization of HNO_3 is strengthened as more water molecules are involved in the clusters.

TABLE 3: Some Bond Lengths (in Å) and Bond Angles (in deg) of $HONO_2 \cdot (H_2O)_\alpha$ $\alpha = 1$ (a), 2 (b), 3 (c) at the HF/6-31G(d) Level[a]

	a	b	c		a	b	c
O_1-N_2	1.195	1.194	1.194	$\angle O_1N_2O_3$	127.6	127.4	127.4
N_2-O_3	1.175	1.177	1.178	$\angle O_1N_2O_4$	117.0	117.1	117.2
N_2-O_4	1.319	1.316	1.315	$\angle N_2O_4H_5$	107.0	107.3	107.4
O_4-H_5	0.972	0.979	0.981	$\angle O_4H_5O_6$	174.7	179.3	179.8
H_5-O_6	1.768	1.703	1.686	$\angle H_5O_6H_7$	101.9	105.2	105.6
O_6-H_7	0.950	0.949	0.950	$\angle H_5O_6H_8$	123.0	119.3	118.9
O_6-H_8	0.949	0.957	0.960	$\angle O_6H_8O_9$		179.9	179.9
H_8-O_9		1.913	1.850	$\angle H_8O_9H_{10}$		118.2	114.8
O_9-H_{10}		0.948	0.956	$\angle H_8O_9H_{11}$		121.5	120.4
O_9-H_{11}		0.948	0.948	$\angle O_9H_{11}O_{12}$			179.3
$H_{11}-O_{12}$			1.926	$\angle H_{11}O_{12}H_{13}$			116.8
$O_{12}-H_{13}$			0.948	$\angle H_{11}O_{12}H_{14}$			117.7
$O_{12}-H_{14}$			0.948				

[a] Refer to Figure 1 for the numbering of atoms.

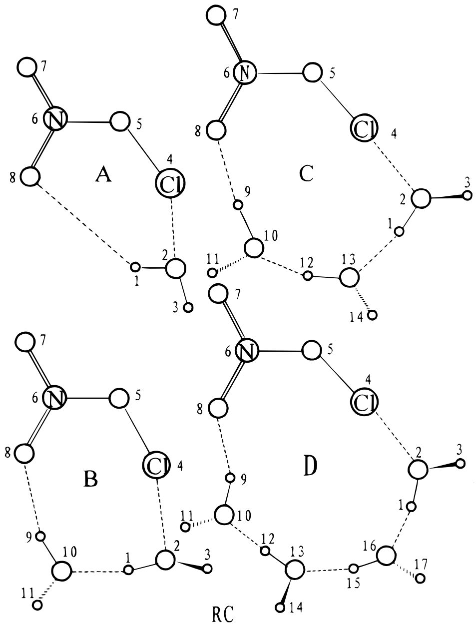

Figure 2. Optimized geometries of $ClONO_2 \cdot (H_2O)_\alpha \cdot H_2O$ (RC), $\alpha = 0$ (A), 1 (B), 2 (C), and 3 (D) at the HF/6-31G(d) level.

Reactant compLex, Product Complex, and Transition-State Structures. Figures 2, 3, and 4 show the optimized geometries of RC, PC, and TS for the reactions of $ClONO_2$ with (A) H_2O, (B) $H_2O \cdot H_2O$, (C) $H_2O \cdot H_2O \cdot H_2O$, and (D) $H_2O \cdot H_2O \cdot H_2O \cdot H_2O$ at the HF/6-31G(d) level. Some of their bond lengths and bond angles are presented in Tables 4 and 5. The structures of the NO_3 group in all of the TS are almost kept the same, and similar results are observed in all of the RC and PC. In the clusters of $HONO_2 \cdot (H_2O)_\alpha HOCl$, the values of r_{O8-H9} are 0.964, 0.978, 0.981, and 0.985 Å, whereas those of r_{H9-O10} are 1.892, 1.721, 1.685, and 1.669 Å for the A, B, C, and D configurations, respectively. Similar to the above result, the change indicates that the ionization of HNO_3 is strengthened as more water molecules are involved in the $HONO_2 \cdot (H_2O)_\alpha HOCl$ clusters. Table 5 presents the comparison of the RC and TS geometries at $\alpha = 2$ between the prediction of the HF/6-31G** of GAMESS[26] and that of our HF/6-31G(d) level. Except for the $H_{11}-O_{10}$ bond length at TS (we suspect that the value in ref 26

TABLE 4: Some Bond Lengths (in Å) and Bond Angles (in deg) of $ClONO_2 \cdot (H_2O)_\alpha \cdot H_2O$ (RC), $[ClONO_2 \cdot (H_2O)_\alpha \cdot H_2O]^\ddagger$ (TS), $HONO_2 \cdot (H_2O)_\alpha \cdot HOCl$ (PC), $\alpha = 0$ (A), 1 (B), and 3 (D) at the HF/6-31G(d) Level[a]

	RC			TS			PC		
	A	B	D	A	B	D	A	B	D
H_1-O_2	0.948	0.956	0.952	0.977	1.262	1.221	1.892	2.002	
O_2-H_3	0.948	0.948	0.947	0.961	0.953	0.953	0.954	0.956	0.951
O_2-Cl_4	2.682	2.593		1.802	1.800	1.805	1.669	1.668	1.670
Cl_4-O_5	1.676	1.681	1.682	2.376	2.108	2.087	4.183	3.989	3.436
O_5-N_6	1.360	1.353	1.350	1.251	1.259	1.263	1.195	1.200	1.200
N_6-O_7	1.175	1.173	1.172	1.192	1.185	1.185	1.172	1.172	1.175
N_6-O_8	1.175	1.182	1.182	1.242	1.236	1.231	1.322	1.312	1.308
$O_8-H_9(H_1)$		2.443	2.186	2.262	1.732	1.944	0.964	0.978	0.985
H_9-O_{10}		0.950	0.950		0.989	0.957	1.892	1.721	1.669
$O_{10}-H_{11}$		0.948	0.948		0.953	0.948		0.948	0.948
$O_{10}-H_{12}(H_1)$		1.971	1.903		1.155	1.812		0.954	0.964
$H_{12}-O_{13}$			0.957			0.964			1.825
$O_{13}-H_{14}$			0.947			0.948			0.948
$O_{13}-H_{15}$			1.837			1.650			0.958
$H_{15}-O_{16}$			0.962			0.987			1.906
$O_{16}-H_{17}$			0.949			0.96			0.947
$\angle Cl_4O_5N_6$	116.1	115.7	116.5	99.4	112.3	113.2	119.3	159.3	168.6
$\angle O_5N_6O_8$	118.8	119.0	119.0	119.9	120.1	118.8	116.8	117.3	117.1
$\angle O_5N_6O_7$	111.4	112.0	112.1	119.6	118.8	118.9	127.9	127.0	126.9
$\angle N_6O_8H_9$	108.2	143.1	160.2	135.6	139.2	116.2	106.7	108.2	108.2
$\angle O_8H_9O_{10}$	169.8	170.9	179.5	129.0	172.2	172.9	167.8	174.6	175.7
$\angle H_9O_{10}H_{11}$	106.1	106.0	105.9	108.8	108.6	105.9	122.6	120.6	119.2
$\angle H_9O_{10}H_{12}$		106.1	112.6		109.2	112.0		112.8	118.5

[a] Refer to Figures 2, 3, and 4 for the numbering of atoms.

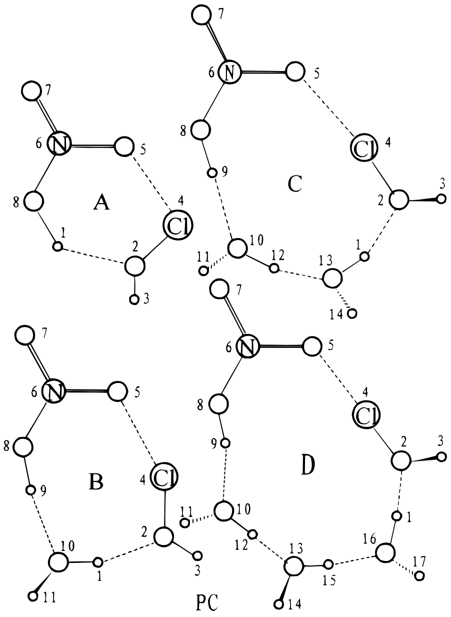

Figure 3. Optimized geometries of $HONO_2 \cdot (H_2O)_\alpha \cdot HOCl$ (PC), $\alpha = 0$ (A), 1 (B), 2 (C), and 3 (D) at the HF/6-31G(d) level.

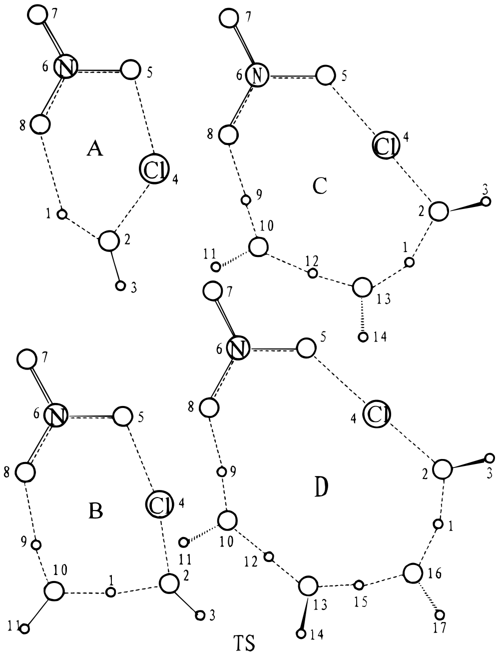

Figure 4. Optimized geometries of $[ClONO_2 \cdot (H_2O)_\alpha \cdot H_2O]^\ddagger$ (TS), $\alpha = 0$ (A), 1 (B), 2 (C), and 3 (D) at the HF/6-31G(d) level.

is a typo), all other bond lengths of RC and TS are very similar. The bond angles of the two computations are also in accordance.

b. Adsorption Energies of Reactants and Products. Figure 5 presents the relative energies of various species with ZPE correction for the reactions of $ClONO_2$ with (A) H_2O, (B) $H_2O \cdot H_2O$, (C) $H_2O \cdot H_2O \cdot H_2O$, and (D) $H_2O \cdot H_2O \cdot H_2O \cdot H_2O$. The relative energies between R and RC (E_{RC-R}) are -8.8 kcal/mol and -6.3 kcal/mol for the reactions of $ClONO_2$ with $H_2O \cdot H_2O$ and $H_2O \cdot H_2O \cdot H_2O$, respectively. But when $\alpha = 3$, the energy difference between RC and R becomes positive. This indicates that the ring of RC at $\alpha = 3$ is relatively unstable compared with that of the lower α. The experimental estimation on the adsorption energy of $ClONO_2$ on ice surfaces is 6−8 kcal/mol.[9] The good consistency between our calculated results on the clusters of $\alpha = 1$ and 2 and the experimental estimation may indicate that $ClONO_2$ is adsorbed on the ice surface with the pattern shown by the models,[26] and the interaction of $ClONO_2$ with the surface comes mainly from $ClONO_2$ with two nearby surface water molecules. The dissociation energies between PC and P (E_{P-PC}) are 8.8 kcal/mol, 5.7 kcal/mol, and 4.8 kcal/mol for the reactions of $ClONO_2$ with $H_2O \cdot H_2O$, $H_2O \cdot H_2O \cdot H_2O$, and $H_2O \cdot H_2O \cdot H_2O \cdot H_2O$, respectively, whereas the experimental value of the adsorption energy of pure HOCl on ice surfaces is 14 ± 2 kcal/mol.[17] The calculated values are much lower than the experimental value. It may be due to the fact that on the ice surfaces, HOCl interacts with several water molecules. On the other hand, the study of the desorption of the product, HOCl, from the ice surfaces between 150 K and 160 K indicates that HOCl is not strongly bound to solid ice.[31]

TABLE 5: Comparison of Structures of [$ClONO_2·(H_2O)_2·H_2O$] (RC), [$ClONO_2·(H_2O)_2·H_2O$]‡ (TS), and $HONO_2·(H_2O)_2·HOCl$ (PC)[a]

	RC	RC[26]	TS	TS[26]	PC
H_1-O_2	0.960	0.954	1.287	1.256	2.134
O_2-H_3	0.948	0.943	0.951	0.948	0.952
O_2-Cl_4	2.521	2.596	1.789	1.783	1.671
Cl_4-O_5	1.688	1.684	2.110	2.136	3.384
O_5-N_6	1.346	1.348	1.257	1.255	1.194
N_6-O_7	1.172	1.173	1.189	1.191	1.177
N_6-O_8	1.184	1.184	1.226	1.228	1.315
O_8-H_9	2.159	2.207	1.775	1.772	0.981
H_9-O_{10}	0.950	0.946	0.968	0.963	1.685
$O_{10}-H_{11}$	0.948	0.943	0.949	0.999	0.949
$O_{10}-H_{12}$	1.898	1.942	1.542	1.537	0.959
$H_{12}-O_{13}$	0.957	0.952	1.008	0.999	1.885
$O_{13}-H_{14}$	0.948	0.943	0.953	0.948	0.948
$O_{13}-H_1$	1.864	1.911	1.113	1.123	0.952
$\angle Cl_4O_5N_6$	116.7	116.7	119.8	121.0	109.9
$\angle O_5N_6O_8$	119.2	119.0	119.3	119.1	117.2
$\angle O_5N_6O_7$	112.2	112.4	118.9	119.2	127.2
$\angle N_6O_8H_9$	154.0	156.0	139.7	146.1	107.1
$\angle O_8H_9O_{10}$	169.6	171.0	165.6	170.2	179.9
$\angle H_9O_{10}H_{11}$	106.0	107.1	105.6	107.4	108.2
$\angle H_9O_{10}H_{12}$	114.5		115.3		118.9
$\angle O_{10}H_{12}O_{13}$	171.8		172.7		179.4
$\angle H_{12}O_{13}H_{14}$	106.0		108.1		114.6
$\angle H_{12}O_{13}H_1$	105.6		110.0		111.4
$\angle O_{13}H_1O_2$	173.3		170.7		150.1
$\angle H_1O_2H_3$	106.1	107.4	119.5	118.2	131.2
$\angle O_2Cl_4O_5$		178.4		179.2	
$\angle Cl_4O_2H_1$		112.1		107.2	

[a] Refer to Figures 2, 3, and 4 (C) for the numbering of atoms. Bond length in Å, bond angle in deg.

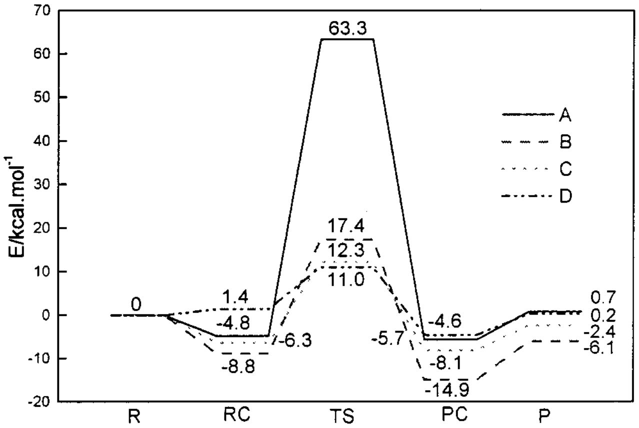

Figure 5. ZPE-corrected relative energies of various species for reactions of $ClONO_2$ with (A) H_2O, (B) $H_2O·H_2O$, (C) $H_2O·H_2O·H_2O$, and (D) $H_2O·H_2O·H_2O·H_2O$ at the MP2//HF/6-31G(d) level of theory. See Figures 2, 3, and 4 for structures. Reactants are taken to be references.

It could be possible that the HOCl formed from the reaction did not have the chance to assume the geometry of the strongest interaction with water molecules before it desorbed from the surface, because of the low temperature at which product was formed. Oppliger et al.[38] reported the formation of a precursor of the product, HOCl, from the reaction of $ClONO_2$ on the ice surface at 160 K. This precursor does not react whereas HCl, while HOCl adsorbed on a pure ice surface reacts readily with HCl under the same conditions. Oppliger et al.[38] also pointed out that the thermally unstable HOCl precursor must be stored in a molecular structure that is very similar to the one in the gas phase. According to our calculation the precursor can be identified to be the PC (or RC).[33] This explanation is the same as that of Berland et al.[27] and that of Bianco and Hynes.[26]

c. Barrier Height of Reaction. The barrier energy is defined as the relative energy between RC and TS (E_{TS-RC}). Our calculation predicts that in the gas phase (α, $\beta = 0$) the barrier energy of the reaction of $ClONO_2$ with H_2O is 68.1 kcal/mol. This is consistent with the experimental observation that the reaction rate is small in the gas phase. The conclusion made here confirmed the calculation of the reaction of $ClONO_2$ with H_2O by Akhmatskaya et al.[22b] They found that the barrier was high in the gas phase for the reaction. When α increases, the barrier energy reduces from 68.1 kcal/mol for $ClONO_2$ with H_2O to 26.2 kcal/mol with $H_2O·H_2O$, to 18.6 kcal/mol with $H_2O·H_2O·H_2O$, and to 9.6 kcal/mol with $H_2O·H_2O·H_2O·H_2O$ (Figure 5). The change of structure leads to the change of barrier energy. Such a catalytic effect of the structure was referred to as structure catalysis.[29,30,33] The barrier height of the reaction mainly comes from the old bond breaking and new bond forming. The geometry of the transition state is also an important factor. If the arrangement of atoms at the transition state is less strained, and the old bond breaking and new bond forming occur almost simultaneously, it is expected that the barrier height can be reduced. The water molecules in the ring provide a bridge to release the stress at the transition state and to help the hydrogen transmission.

B. Hydration and Ionization. Because the barrier energy of reaction 1 with the ring only is too high to account for the fast rate of reaction on ice surfaces at low temperature, we have to consider the possibility that hydration of the ring will reduce the barrier further, as was done by Bianco and Hynes.[26] According to the MTS model, the core of $ClONO_2$ hydrolysis on ice surfaces is the ring of $ClONO_2·H_2O·(H_2O)_\alpha$, where $ClONO_2$ and H_2O are reactants, $\alpha = 2$ or 3. Bianco and Hynes[26] pointed out that in the case of the $ClONO_2$ reaction on ice surfaces, $\alpha = 2$ is the most likely case that an ice surface will provide. Although the barrier height at $\alpha = 3$ is lowest among the calculated geometries, for the reasons mentioned above and to avoid computational difficulty, we chose $\alpha = 2$ for further investigation.

Different positions of hydration are designed and calculated with the same method as above. Figure 6 presents just the transition state structures of the reactions of various considerations. Some optimized bond lengths are listed in Table 6. The optimized bond lengths and angles of water molecules are similar to those of the ice structure (I_h). In the I_h ice the bond lengths of O−H and H- -O are 0.97 Å and 1.79 Å, respectively, and the bond angles of ∠OOO and ∠HOH are 109.5° and 104.5°, respectively.[39]

To focus on the effect of the neighboring molecules on the reaction, we now concentrate on the RC, TS, and PC relative energies. The ZPE-corrected relative energies for the reactions of $ClONO_2·(H_2O)_2·H_2O·(H_2O)_\beta$, $\beta = 0,1,2$ are shown in Figure 7. The barrier energies decrease when β is increased. When $\beta = 1$, the barrier energy of the F configuration is 3.9 kcal/mol, the lowest value among the three (E, F, G) configurations, whereas the barrier energy of the E configuration is at the middle, 11.6 kcal/mol. When $\beta = 2$ for the H configuration, the barrier energy is 3.2 kcal/mol. The calculation confirmed the result by Bianco and Hynes on the reaction of $ClONO_2$ with nH_2O.[26] It is worth pointing out that all the calculations so far have only considered water molecules outside of the ring being proton acceptors. In ice there are also water molecules that attach to the ring as proton donors. These molecules also affect the reaction, although the effect is expected to be smaller, as was found by us in other systems.[40] Further study with more water

TABLE 6: Some Bond Lengths (in Å) of $ClONO_2\cdot(H_2O)_2\cdot H_2O\cdot(H_2O)_\beta$ (RC), $[ClONO_2\cdot(H_2O)_2\cdot H_2O\cdot(H_2O)_\beta]^\ddagger$ (TS), and $HONO_2\cdot(H_2O)_2\cdot HOCl\cdot(H_2O)_\beta$ (PC), $\beta = 1$ (E, F, G) and 2(H) at the HF/6-31G(d) Level[a]

	E			F			G			H		
	RC	TS	PC	RC	TS	PC	RC	TS	PC	RC	TS	PC
O_2-Cl_4	2.526	1.796	1.692	2.495	1.814	1.671	2.498	1.737	1.669	2.494	1.807	1.671
Cl_4-O_5	1.689	2.111	3.433	1.697	2.074	3.428	1.696	2.271	3.442	1.697	2.085	3.424
O_5-N_6	1.347	1.255	1.199	1.343	1.258	1.197	1.343	1.245	1.196	1.343	1.257	1.200
N_6-O_8	1.182	1.228	1.306	1.182	1.235	1.315	1.183	1.234	1.314	1.182	1.227	1.305
N_6-O_7	1.175	1.189	1.177	1.176	1.184	1.177	1.175	1.194	1.177	1.176	1.188	1.177
O_8-H_9	2.254	1.940	0.996	2.234	1.989	0.984	2.227	1.754	0.982	2.234	1.909	0.995
H_9-O_{10}	0.949	0.958	1.608	0.950	0.957	1.671	0.950	0.971	1.682	0.949	0.958	1.608
$H_{11}-O_{15}$	1.973	1.958	1.911							1.972	2.004	1.932
H_3-O_{15}							1.988	1.779	1.836			
$H_{14}-O_{15}$				1.977	1.782	1.956						
$H_{14}-O_{18}$										1.977	1.843	1.967

[a] Refer to Figure 6 for the numbering of atoms.

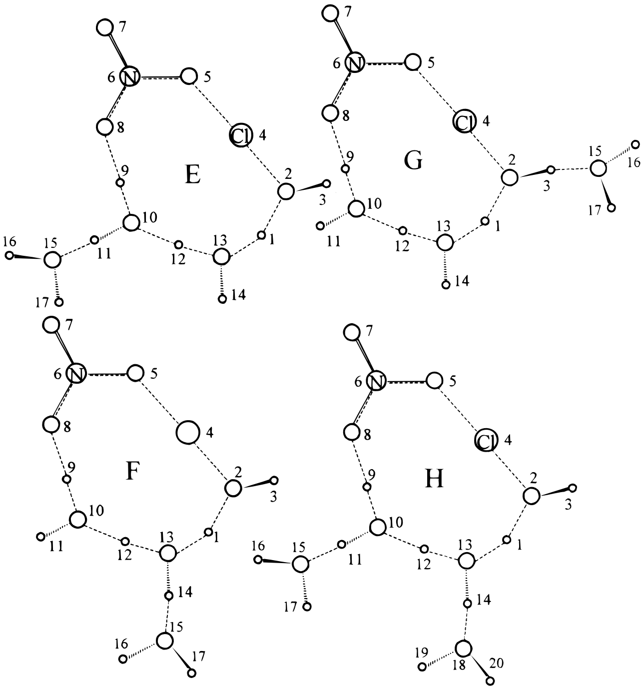

Figure 6. Optimized structures of $ClONO_2\cdot(H_2O)_2\cdot H_2O\cdot(H_2O)_\beta$ (TS), $\beta = 1$ (E), $\beta = 1$ (F), $\beta = 1$ (G), and $\beta = 2$ (H) at the HF/6-31G(d) level.

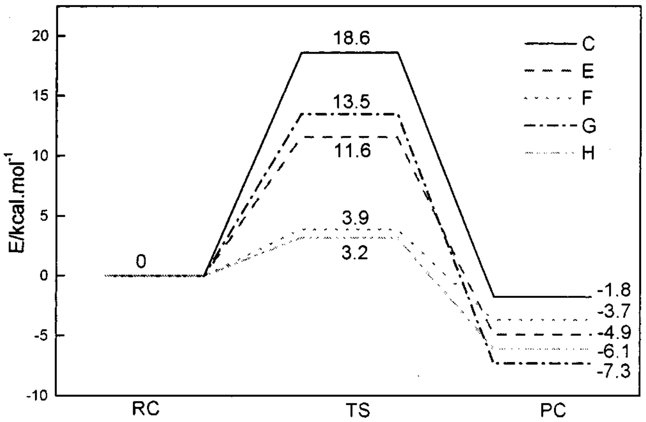

Figure 7. ZPE-corrected relative energies of various species for reactions of $ClONO_2\cdot(H_2O)_2\cdot H_2O\cdot(H_2O)_\beta$, $\beta = 0$ (C), $\beta = 1$ (E), $\beta = 1$ (F), $\beta = 1$ (G), and $\beta = 2$ (H) at the MP2//HF/6-31G(d) level of theory. See Figures 2, 3, 4, and 6 for structures. Reactant complexes are taken to be references.

TABLE 7: Electric Charges of Some Atoms and Groups at the HF/6-31G(d) Level[a,b]

	RC	TS	PC		RC	TS	PC
A Cl_4	0.367	0.496	0.266	E Cl_4	0.388	0.420	0.239
O_2H_3	−0.424	−0.236	−0.246	O_2H_3	−0.502	−0.422	−0.230
H_1	0.452	0.576	0.545	H_9	0.479	0.524	0.570
NO_3[c]	−0.395	−0.834	−0.564	NO_3[c]	−0.434	−0.780	−0.640
B Cl_4	0.375	0.399	0.232	F Cl_4	0.392	0.424	0.242
O_2H_3	−0.484	−0.408	−0.223	O_2H_3	−0.505	−0.410	−0.235
H_9	0.479	0.597	0.565	H_9	0.488	0.510	0.568
NO_3[c]	−0.415	−0.773	−0.603	NO_3[c]	−0.442	−0.760	−0.624
C Cl_4	0.390	0.406	0.246	G Cl_4	0.394	0.369	0.207
O_2H_3	−0.502	−0.431	−0.240	O_2H_3	−0.502	−0.361	−0.229
H_9	0.497	0.554	0.567	H_9	0.492	0.550	0.566
NO_3[c]	−0.434	−0.788	−0.617	NO_3[c]	−0.448	−0.833	−0.619
D Cl_4	0.381	0.403	0.208	H Cl_4	0.392	0.427	0.238
O_2H_3	−0.499	−0.412	−0.215	O_2H_3	−0.507	−0.422	−0.230
H_9	0.493	0.507	0.577	H_9	0.476	0.523	0.568
NO_3[c]	−0.418	−0.760	−0.621	NO_3[c]	−0.442	−0.770	−0.640

[a] Refer to Figures 2, 3, 4, and 6 for the numbering of atoms. [b] To make a comparison, the charge distribution of some molecules at the same theoretical level are given as following: $ClONO_2$: Cl, +0.338; NO_3, −0.338. HOCl: Cl, +0.211; OH, −0.211. H_2O: H, +0.434; OH, −0.434. HNO_3: H, +0.493; NO_3, −0.493. [c] Unlike other subscript numbers, which stand for the label of the atom, here NO_3 means the group of one N and three O, the identity of which is obvious.

molecules and full consideration of both proton acceptors and donors is desired.

As clearly shown by the calculation, additional water molecules play an essential role in further reducing the barrier energy of reaction 1. The water molecules not only provide a bridge to the reaction coordinate but also enhance the ionic character of the chemical species involved by changing the charge distributions through hydration. To illustrate this, Table 7 gives the electric charges of some atoms and groups. The reduction of the barrier energy has a clear correlation with the ionic character of important species. The trends of ionization of the involved species are enhanced with more hydration. On the other hand, it is noticed that the TS has a very strong charge separation, and hydration helps to stabilize the ion separation in the TS so that it reduces the reaction barrier. These factors can be displayed by the total change of the charge distribution from RC to TS defined by

$$\Delta\delta = [\sum_i [\delta_{TSi} - \delta_{RCi}]^2]^{1/2}$$

Table 8 lists the values of E_{TS-RC} and $\Delta\delta$. Notice that there is rough correlation between E_{TS-RC} and $\Delta\delta$. To a large extent, we can say that our calculated results are consistent with the mechanism of Sodeau and co-workers.[16,31,32] In reality, the species on ice surfaces at temperature around 200 K or lower could be just partially ionized. They are neither completely independent ions nor free neutral molecular entities. The extent

TABLE 8: Barrier Energy (E_{TS-RC}) in Kcal/Mol, and the Change of Charge Distribution ($\Delta\delta$) between TS and RC

	A	B	C	D	E	F	G	H
$\Delta\delta$	0.360	0.314	0.275	0.272	0.280	0.268	0.304	0.281
E_{TS-RC}	68.1	26.2	18.6	9.6	11.6	3.9	13.5	3.2

of ionization depends on experimental conditions such as the temperature and the ratio of reactants to water. However, there is a slight difference between this model and some other previous ion-catalyzed mechanisms. In some previous ion-catalyzed mechanisms,[9,19−23] the ion comes from outside, but in this mechanism the ion comes naturally from the interaction of reactants themselves with water molecules. It is important to mention that the calculation made here is more appropriate at extremely low temperatures. At higher temperatures, the hydrated species may demonstrate even stronger ionic character, as observed by Sodeau et al.[16,31,32] It is easily understandable that the thermal energy available at high temperature will allow higher mobility of species and more complete hydration of them. This will likely make the ionic character stronger and push the reaction further in the direction of the product thermally and dynamically. Unfortunately, at present it is not possible for us to accurately answer those questions because of our limited computational capability. Further studies certainly are necessary.

Although the direct relation of our calculation is with water clusters, we would like to draw some links to the reaction on ice surfaces. First, we admit that the calculation made on water clusters does not apply directly to the reaction on surfaces. The surface reaction is much more complex. For example, the bond lengths and bond angles may vary from the clusters because of the constraint of the ice bulk and surface structures. As noticed by Bianco and Hynes,[26] going from the clusters to the surfaces, both factors of raising and lowering the barrier exist. Another issue is the entropy factor. In the reaction, $ClONO_2$ is identified as a gas, whereas H_2O is previously formed on the ice surface. The product, HOCl, is identified as a gas, too. The ice surface is quite rigid with almost the correct geometry to accommodate the gas-phase species. Therefore, the entropy effect on the surface reaction is not as great as it is for a gas-phase reaction involving cluster formation. The energetic considerations on clusters can be compared with the surface reaction, but not the entropy consideration.

One result that we think is important from our calculation is that the barrier energy of the reaction depends on the extent of hydration. When the ratio of water:reactant is small, referred to as the reactant-rich condition, the core of the reaction is not fully hydrated, or it even does not have enough water molecules in the ring, so the barrier of the reaction is high. When the ratio of water:reactant is large, referred to as the water-rich condition, we expect to see that the reaction barrier is lower. Barone et al.[28] observed that, at the condition of the ratio of the partial pressures of water:$ClONO_2$ ∼10:1 and 110 K, the reaction of $ClONO_2$ on ice surfaces takes place. They stated explicitly that $ClONO_2$ hydrolysis occurs most efficiently on a water-rich hydrate surface. Sodeau et al.[16] reported that at the condition of the ratio of the partial pressures of $ClONO_2$:water ∼10:1 and 180 K, the reaction of $ClONO_2$ with H_2O did not occur noticeably, whereas upon turning on the flow of water into the chamber the reaction of $ClONO_2$ with H_2O at once took place. These experimental observations may be well explained by the variation of the extent of hydration at different experimental conditions.

Recently, Berland et al. presented surface-sensitive studies of the reactive uptake of chlorine nitrate on ice using laser-induced thermal desorption techniques.[27] They found the reaction probability (γ) for $ClONO_2$ hydrolysis on ice as a function of the negative temperature dependence. $\gamma = 0.03$ was independent of temperature from 75 K to 110 K. At temperatures >110 K, γ decreased with increasing temperature and reached a value of 0.005 at 140 K. A precursor-mediated adsorption model was proposed by them to explain the experimental results. Their model is consistent with our theoretical model, if we identify the precursor in their model as the RC in our calculation. Furthermore, some values calculated here are consistent with their values. For example, they estimated that the reaction barrier is about 3 kcal/mol, which agrees well with the estimation of ∼3−7 kcal/mol[26,41] and our calculated value of 3.2 kcal/mol. The adsorption energy of 7 kcal/mol of the precursor is also close to the absorption energy of $ClONO_2$, 6−8 kcal/mol. Therefore, the theoretical model here can explain their experimentally observed negative temperature dependence of the reaction probability.

Type I PSCs comprise HNO_3 and H_2O in the form of frozen nitric acid trihydrate (NAT) and condense at 195 K in the stratosphere.[42] This is 5−7 K higher than that of type II PSCs, which are composed mainly of water ice. Because HNO_3 binds strongly to the water molecules in the ice, the formation of MTS for the reaction is hindered and the hydration effect of water is reduced. The MTS mechanism predicts that the reaction rate on NAT surfaces will be lower than that on pure ice surfaces.[25,26,33] Experimental results show that γ of $ClONO_2$ on NAT is two orders of magnitude smaller than that on type II surfaces.[15]

IV. Conclusion

The MP2//HF/6-31G(d) level calculation on the model reaction has shown that as more water molecules are involved in the $ClONO_2$ hydrolysis, the barrier height drops dramatically. The barrier energies of the reaction on the water clusters vary with the extent of hydration. A value as low as 3.2 kcal/mol was observed in the calculation. Through this study, it has been implied that the surface of ice catalyzes the heterogeneous reaction through structure catalysis and hydration. The models of the structure-catalyzed and ion-catalyzed mechanisms can be put together to explain the experimental observations.

Acknowledgment. This work was supported by the Ministry of Science and Technology of China through the Climbing Projects and by NSFC. Parts of the calculations were done at power challenge computer of CSTNETSERVER.

References and Notes

(1) Farman, J. C.; Gardiner, B. G.; Shanklin, J. D. *Nature* **1985**, *315*, 207.

(2) Solomon, S.; Garcia, R. R.; Rowland, F. S.; Wuebbles, D. J. *Nature* **1986**, *321*, 755.

(3) Crutzen, P. J.; Arnold, F. *Nature* **1986**, *324*, 651.

(4) Rowland, F. S. *Annu. Rev. Phys. Chem.* **1991**, *42*, 731.

(5) Molina, M. J.; Molina, L. T.; Kolb, C. E. *Annu. Rev. Phys. Chem.* **1996**, *47*, 327.

(6) Abbatt, J. P. D.; Molina, M. J. *J. Phys. Chem.* **1992**, *96*, 7674.

(7) Hanson, D. R.; Mauersberger, K. *J. Phys. Chem.* **1988**, *92*, 6167.

(8) McElrory, M. B.; Salawitch, R. J.; Wofsy, S. C. *Geophys. Res. Lett.* **1986**, *13*, 1296.

(9) Molina, M. J.; Tso, T. L.; Molina, L. T.; Wang, F. C. Y. *Science* **1987**, *238*, 1253.

(10) Tolbert, M. A.; Rossi, M. J.; Malhotra, R.; Golden, D. M. *Science* **1987**, *238*, 1258.

(11) Steele, H. M.; Hamill, P.; McCormick, M. P.; Swissler, T. J. *J. Atmos. Sci.* **1983**, *40*, 2055.

(12) Brune, W. H.; Anderson, J. G.; Toohey, D. W.; Fahey, D. W.; Kawa, S. R.; Jones, R. L.; McKenna, D. S.; Poole, L. R. *Science* **1991**, *252*, 1260.

(13) DeMore, W. B.; Sander, S. P.; Golden, D. M.; Hampson, R. F.; Kurylo, M. J.; Howard, C. J.; Ravishankara, A. R.; Kolb, C. E.; Molina, M. J. *Chemical Kinetics and Photochemical Data for Use in Stratospheric Modeling*; Evaluation No. 10; NASA, Jet Propulsion Laboratory: Pasadena, CA, 1992; Publ. 92−20.

(14) Leu, M. T. *Geophys. Res. Lett*. **1988**, *15*, 17.

(15) DeMore, W. B.; Sander, S. P.; Golden, D. M.; Hampson, R. F.; Kurylo, M. J.; Howard, C. J.; Ravishankara, A. R.; Kolb, C. E.; Molina, M. J. *Chemical Kinetics and Photochemical Data for Use in Stratospheric Modeling*; Evaluation No. 12; NASA, Jet Propulsion Laboratory: Pasadena, CA, 1997; Publ. 97−4.

(16) Sodeau, J. R.; Horn, A. B.; Banham, S. F.; Koch, T. G. *J. Phys. Chem.* **1995**, *99*, 6258.

(17) Hanson, D. R.; Ravishankara, A. R. *J. Phys. Chem*. **1992**, *96*, 2682.

(18) Banham, S. F.; Horn, A. B.; Koch, T. G.; Sodeau, J. R. *Faraday Discuss*. **1995**, *100*, 321.

(19) Wofsy, S. C.; Molina, M. J.; Salawitch, R. J.; Fox, L. E.; McElroy, M. B. *J. Geophys. Res*. **1988**, *93*, 2442.

(20) Lee, T. J.; Rice, J. E. *J. Phys. Chem*. **1993**, *97*, 6637.

(21) Nelson, C. M.; Okumura, M. *J. Phys. Chem*. **1992**, *96*, 6112.

(22) (a) Mebel, A. M.; Morokuma, K. *J. Phys. Chem*. **1996**, *100*, 2985. (b) Akhmatskaya, E. V.; Apps, C. J.; Hillter, L. H.; Masters, A. J.; Palmer, L. J.; Watt, N. E.; Vincent, M. A.; Whitehead, J. C. *J. Chem. Soc., Faraday Trans*. **1997**, *93*, 2775.

(23) Gertner, B. J.; Hynes, J. T. *Science* **1996**, *271*, 1563.

(24) Hanson, D. R. *J. Phys. Chem*. **1995**, *99*, 13059.

(25) Ying, L. M.; Zhao, X. S. *J. Phys. Chem. A* **1997**, *101*, 6807.

(26) (a) Bianco, R.; Hynes, J. T. *J. Phys. Chem. A* **1998**, *102*, 309. (b) Bianco, R.; Gertner, B. J.; Hynes, J. T. *Ber. Bunsen-Ges. Phys. Chem.* **1998**, *102*, 518.

(27) Berland, B. S.; Tolbert, M. A.; George, S. M. *J. Phys. Chem. A* **1997**, *101*, 9954.

(28) Barone, S. B.; Zondlo, M. A.; Tolbert, M. A. *J. Phys. Chem. A* **1997**, *101*, 8643.

(29) Xu, S. C.; Zhao, X. S. Proceedings of Symposium on Frontiers of Chemistry-2nd CWCYC, Hong Kong, 1997; P540.

(30) Xu, S. C.; Zhao, X. S. *Acta Phys. Chim. Sin.* **1998**, *14*, 5.

(31) Horn, A. B.; Sodeau, J. R.; Roddis, T. B.; Williams, N. A. *J. Phys. Chem. A* **1998**, *102*, 6107.

(32) Horn, A. B.; Sodeau, J. R.; Roddis, T. B.; Williams, N. A. *J Chem. Soc., Faraday Trans.* **1998**, *94*, 1721.

(33) Xu, S. C.; Zhao, X. S. *Acta Phys. Chim. Sin.* **1998**, *14*, 988.

(34) Frisch, M. J. et al. Gaussian 94, Revision B. 3, Gaussian, Inc.: Pittsburgh, PA, 1995.

(35) Lee, T. J. *J. Phys. Chem*. **1995**, *99*, 1943.

(36) (a) Cox, A. P.; Riveros, J. M. *J. Chem. Phys*. **1965**, *42*, 3106. (b) Casper, B.; Lambotte, P.; Minkwitz, R.; Oberhammer, H. *J. Phys. Chem*. **1993**, *97*, 9992.

(37) Xantheas, S. S.; Dunning, T. H., Jr. *J. Chem. Phys*. **1993**, *99*, 8774.

(38) Oppliger, R.; Allanic, A.; Rossi, M. J. *J. Phys. Chem. A*, **1997**, *101*, 1903.

(39) Zhou, G. *Fundamental of Structure Chemistry*; World Scientific Company: Singapore, 1993.

(40) Xu, S. C.; Zhao, X. S. *Acta Phys. Chim. Sin.*, in press.

(41) Tabazadeh, A.; Turco, R. P. *J. Geophy. Res*. **1993**, *98* (*D7*), 12727.

(42) Moore, S. B.; Keyser, L. F.; Leu, M.-T.; Turco, R. P.; Smith, R. H. *Nature* **1990**, *345*, 333.